

Dual-energy imaging performance of sandwich detectors with fiber-optic faceplate

Dong Woon Kim ^a, Junwoo Kim ^a, Jiwoong Park ^a, Ho Kyung Kim ^{a,b*}

^a School of Mechanical Engineering, Pusan National University, Busan, Republic of Korea

^b Center for Advanced Medical Engineering Research, Pusan National University, Busan, Republic of Korea

*Corresponding author: hokyung@pusan.ac.kr

1. Introduction

Dual-energy imaging (DE) technique enhances the material to be viewed using two images acquired from low- and high-energy [1,2]. Since the DE images are acquired through two exposure, motion artifacts occur due to the patient's motion, respiration, and heartbeat. To solve this motion artifact problem, single-shot DE method using a sandwich-like multilayer detector has been proposed [3]. The sandwich detector generates beam-hardening from an intermediate filter between the two detector layers to produce energy-separated images of low- and high-energy [4,5].

The incident x-rays reaching the photodiode array do not largely affect the detector signal but have a bad influence on the noise and damage the photodiode array. To prevent this, the fiber-optic faceplate (FOP) is located between the scintillator and the photodiode array, the FOP keeps the signal from scintillator and minimizes the direct response of the incident x-rays to the photodiode array [6-8].

In this study, we try to improve the detector performance by inserting the FOP in the front detector of the sandwich detector to induce energy separation by replacing the intermediate filter.

2. Theoretical background

2.1 Sandwich detector with FOP

In previous study, the sandwich detector was theoretically modeled using cascaded-systems model (CSA) [9,10], and the performance of the sandwich detector for various kVp and intermediate filter thickness was analyzed[5]. The x-ray transmitted through the front detector and the intermediate filter reaches the rear detector, and the image corresponding to the relatively higher energy can be obtained the rear detector. Transmission is one of the important factors because the rear detector of sandwich detector acquires images using attenuation. The direct interaction of the photodiode array indicates that it reacts directly to the photodiode

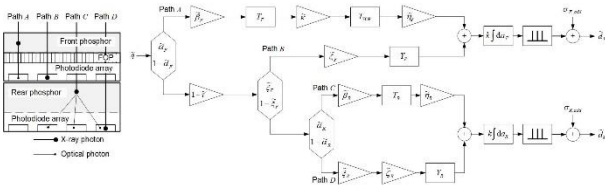


Fig. 1. A schematic diagram and cascaded-model block diagram describing signal and noise propagation in the flat-panel sandwich detector with fiber-optic faceplate.

array from x-ray transmission. The direct interaction increases the noise of the image in the form of white noise, so it works especially in the high frequency region. To reduce this direct interaction, the FOP is placed between the scintillator and the photodiode array in front detector. Also, since the image of rear detector requires a relatively high-energy image from the beam-hardening, it is considered that the FOP can replace the intermediate filter. Fig. 1 shows a schematic diagram of a sandwich detector with FOP and a block diagram proposed in this study describing signal and noise propagation from the incident x-ray.

In this study, the signal and noise propagation of the sandwich detector is modeled through four paths in consideration of the direct interaction. Path A describes conversion of x-ray quanta to optical quanta in the front phosphor and their detection in the front photodiode array. Path B describes detection of charge carriers liberated by direct interactions in the photodiode array. Path C describes charge carriers liberated in the rear detector from x-ray interactions in the rear phosphor and path D describes direct x-ray interactions in the rear photodiode.

2.2 Cascaded-systems model

The CSA was used to obtain detector signal and noise power spectrum (NPS) considering the gain \bar{d} and spread by scintillator and photodiode from incident x-ray \bar{q} (quanta mm^{-2}). It is modeled using a $\text{Gd}_2\text{O}_2\text{S:Tb}$ phosphor screen (Carestream Health Inc., Rochester, NY) and a photodiode array (RadEye1™, Teledyne Rad-Icon Imaging Corp., Sunnyvale, US) having 512×1024 pixels with a pixel pitch (p) 0.048 mm. In addition, 1 mm and 2 mm FOPs were used in order to reduce the effects of direct interaction and beam-hardening.

The signal of the detector that inserted the FOP is as follows:

$$\bar{d} = k\alpha^2\bar{q}(\bar{m}_{\text{indirect}} + \bar{m}_{\text{direct}}) = k\alpha^2\bar{q}(\bar{\alpha}\bar{\beta}\bar{\kappa}\eta + \hat{\alpha}\hat{\tau}\bar{\xi}\bar{\zeta}) \quad (1)$$

where gain $\bar{m}_{\text{indirect}}$ of scintillator consists of quantum efficiency $\bar{\alpha}$ of scintillator for the incident x-ray, conversion gain $\bar{\beta}$ of light photon by FOP, and light quantum efficiency η of photodiode array. Gain \bar{m}_{direct} of photodiode array consists of transmittance $\hat{\alpha}$ of scintillator, transmittance $\hat{\tau}$ of FOP, quantum efficiency $\bar{\xi}$ of photodiode array for the incident x-ray, and charge carriers conversion gain $\bar{\zeta}$. k denotes scaling factor from charge carriers (e^-) to

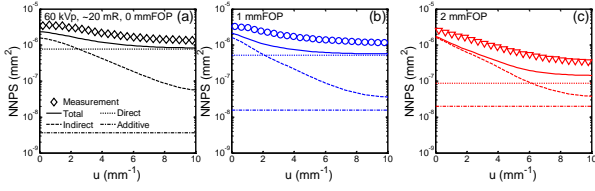


Fig. 2. NNPS of detector with FOP for various FOP thicknesses. (a) without FOP, (b) 1 mm FOP, and (c) 2 mm FOP.

output detector signal in digital units (DN) and a denotes photosensitive aperture pitch.

Presampling 1D NPS is as follows:

$$W^*(u) = k^2 a^4 \bar{q} \left[\bar{m}_{\text{indirect}}^2 \left\{ \frac{1}{\bar{m}_{\text{indirect}}} + \frac{1}{\bar{\alpha}} \left(\frac{1}{I_{\text{indirect}}} - \frac{1}{\beta} \right) T^2(u) \right\} + \bar{\alpha} \bar{m}_{\text{direct}}^2 \left\{ \frac{1}{\bar{m}_{\text{direct}}} + \frac{1}{\bar{\xi}} \left(\frac{1}{I_{\text{direct}}} - \frac{1}{\zeta} \right) Y^2(u) \right\} \right] \sin^2(\pi a u) \quad (2)$$

where I denotes swank noise factor, T and Y denote modulation transfer function (MTF) in scintillator and photodiode array, respectively. The detective quantum efficiency (DQE) can be expressed as,

$$DQE(u) = \frac{\bar{d}^2 MTF^2(u)}{\bar{q} NPS(u)} = \frac{MTF^2(u)}{\bar{q} [NPS(u)/\bar{d}^2]} \quad (3)$$

3. Preliminary results

Fig. 2 shows normalized NPS (NNPS) for various FOP thicknesses. As the FOP thickness is increased, the noise due to the direct interaction is much reduced and the overall NNPS is reduced. In particular, the noise components in the high frequency region are much improved due to the reduction of direct interaction noise acting as white noise.

Fig. 3(a) shows response of detector with FOP for various FOP thicknesses. When the FOP is inserted between scintillator and photodiode array, the detector signals are about twice as low as when there is without FOP. It can be seen that as the FOP thickness increases, the detector signal decrease, but the detector signal decreases slightly as the thickness increases from 1 mm to 2 mm. Fig. 3(b) shows MTF of detector with FOP for various FOP thicknesses. It can be seen that the MTF is reduced by the FOP but the MTF is hardly changed by the FOP thicknesses. As shown in Fig. 3(c), the DQE is lowered when the FOP is 1 mm, but the DQE is better when the FOP is 2 mm as compared with the case without the FOP. This means that the FOP thickness is related to the performance of the detector.

In this study, the performance of detector with FOP is modeled theoretically and the detector performance according to FOP thickness is confirmed. From the results, it can be seen that there is a decrease of the signal according to the FOP thickness, but the signal is not greatly decreased according to the FOP thickness, and it is confirmed that the noise due to the direct interaction is improved relatively. It seems that the FOP is used instead of intermediate filter for energy separation could obtain a better single-shot DE image with sufficient energy separation and reduced direct interaction noise.

4. Further Studies

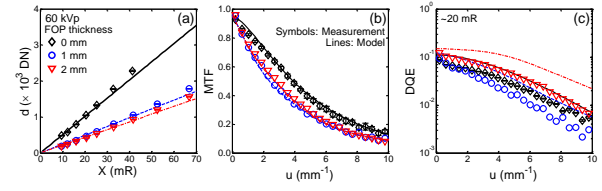


Fig. 3. Performance of detector with FOP for various FOP thicknesses. (a) Response, (b) MTF, and (c) DQE..

We plan to further study the following subjects based on the theoretical model of sandwich detector with FOP.

- Theoretical modeling of sandwich detectors with FOP.
- Single-shot DE image performance analysis by various FOP thicknesses.

ACKNOWLEDGEMENT

This work was supported by the National Research Foundation of Korea (NRF) grants funded by the Korea governments (MSIP) (No. 2017M2A2A6A01019930).

REFERENCES

- [1] R. E. Alvarez, J. A. Seibert, and S. K. Thompson, Comparison of dual energy detector system performance, *Med. Phys.*, Vol. 31, No. 3, pp. 556-565, 2004.
- [2] S. Richard and J. H. Siewerdsen, Optimization of dual-energy imaging systems using generalized NEQ and imaging task, *Med. Phys.*, Vol. 34, No. 1, pp. 127-139, 2007
- [3] S. Yun, J. C. Han, D. W. Kim, H. Youn, H. K. Kim, J. Tanguay, and I. A. Cunningham, Feasibility of active sandwich detectors for single-shot dual-energy imaging, *Proc. SPIE 9033*, p. 90335T, 2014.
- [4] D. W. Kim, H. K. Kim, H. Youn, S. Yun, J. C. Han, J. Kim, S. Kam, J. Tanguay, and I. A. Cunningham, Signal and noise analysis of flat-panel sandwich detectors for single-shot dual-energy x-ray imaging, *Proc. SPIE 9413*, p. 94124A-1, 2015.
- [5] D. W. Kim, J. Kim, S. Yun, H. Youn, and H. K. Kim, Cascaded-systems analysis of sandwich x-ray detectors, *J. Instrum.*, Vol. 11, No. 12, p. C12022, 2016
- [6] J. C. Han, S. Yun, C. H. Lim, T. W. Kim, and H. K. Kim, Feasibility study of CMOS detectors for mammography, *Proc. SPIE 7258*, p. 72583I-1, 2009.
- [7] A. Jain, D. Bednarek, C. Ionita, and S. Rudin, A theoretical and experimental evaluation of the microangiographic fluoroscope: A high-resolution region-of-interest x-ray imager, *Med. Phys.*, Vol. 38, No. 7, pp. 4112-4126, 2011.
- [8] C. H. Lim, S. Yun, J. C. Han, H. K. Kim, M. G. Farrier, T. G. Achterkirchen, M. McDonald, and I. A. Cunningham, Characterization of imaging performance of a large-area CMOS active-pixel detector for low-energy x-ray imaging, *Nucl. Instrum. Meth. A*, Vol. 652, No. 1, pp. 500-503, 2011.
- [9] I. A. Cunningham, M. S. Westmore, and A. Fenster, A spatial-frequency dependent quantum accounting diagram and detective quantum efficiency model of signal and noise propagation in cascaded imaging systems, *Med. Phys.*, Vol 21, No. 3, pp. 417-427, 1994.
- [10] J. H. Siewerdsen, L. E. Antonuk, Y. El-Mohri, J. Yorkston, W. Huang, J. M. Boudry, and I. A. Cunningham, Empirical and theoretical investigation of the noise performance of indirect detection, active matrix flat-panel imagers (AMFPIs) for diagnostic radiology, *Med. Phys.*, Vol. 24, No. 1, pp. 71-89, 1997.